

# The Formation of the Cold Classical Kuiper Belt by a Short Range Transport Mechanism

RODNEY GOMES<sup>1</sup>

<sup>1</sup>*Observatório Nacional*

*Rua General José Cristino 77, CEP 20921-400, Rio de Janeiro, RJ, Brazil*

## ABSTRACT

The Classical Kuiper Belt is populated by a group of objects with low inclination orbits, reddish colors and usually belonging to a binary system. This so called Cold Classical Kuiper Belt is considered to have been formed in situ from primordial ice pebbles that coagulated into planetesimals hundreds of kilometers in diameter. According to this scenario, the accretion of pebbles into large planetesimals would have occurred through the streaming instability mechanism that would be effective in the primordial Solar System disk of gas and solids. Nevertheless other objects with the same color characteristics as those found in the Cold Classical Kuiper Belt can be encountered also past the 2:1 mean motion resonance with Neptune as scattered or detached objects. Here I propose a mechanism that can account for both the cold Classical Kuiper Belt objects and other reddish objects outside the Classical Kuiper Belt. According to the proposed scenario, reddish objects were primordially in the outer portion of the planetesimal disk which was however truncated somewhere below  $\sim 42$  au. In this manner the cold Classical Kuiper Belt and its scattered / detached counterpart were respectively transported outwards by a short range or slightly scattered to their present locations. Resonant objects were also formed by the same process. This mechanism is aimed at explaining the distribution of all objects that share the same color characteristics as coming from a common origin in the outer borders of the primordial planetesimal disk. According to the scenario here proposed the Cold Classical Kuiper Belt would have been formed  $\sim 4$  au inside its present location with a total mass 20 – 100 times as large as its present value.

## 1. INTRODUCTION

Trans-Neptunian objects (TNOs) show a conspicuous orbital architecture that is best characterized through the classification of the total population into specific subpopulations known as: the classical Kuiper belt (CKB), cold (CCKB) and hot, the resonant population, the scattered population and the detached popu-

lation. This remarkable orbital distribution into several subpopulations is a consequence of the gravitational interaction of the giant planets and a disk of planetesimals in the early Solar System that accounted for the implantation of the planets on their present orbits and the planetesimals that induced the planets migration onto their several different populations. That process included resonance trapping and evolution in resonance of the planetesimals with the major planets (mainly Nep-

tune) (Malhotra 1995; Gomes 2000), scattering by close encounters with the migrating planets, resonance sticking of scattering planetesimals into mean motion resonances (MMR) and Kozai resonances with Neptune and possible escape from these resonances (Gomes 2003, 2011; Lykawka & Mukai 2007). Among these TNOs subpopulations, the CCKB is presently regarded as the set of objects that experienced the least interactions with the migrating planets.

The CCKB is possibly the part of the Kuiper belt that best represents the TNOs as first conceived by its first proposers (Kuiper 1951; Edgeworth 1949). It is roughly a set of objects with relatively low eccentricity and low inclination orbits and semimajor axes roughly between 42 au and 47 au. Nevertheless, we cannot claim that the eccentricities of the CCKB is as low as expected if these objects were perturbed during the age of the Solar System solely by the planets at their present orbital configurations. It is thus understood that the migrating planets had some influence albeit small on the present CCKB orbits (Nesvorný 2015; Dawson & Murray-Clay 2012; Gomes et al. 2018; Ribeiro de Sousa et al. 2019). This perturbation on the CCKB's objects must have been weak enough in order to avoid not only an excessive excitation of the CCKB orbits but also to preserve their binary feature. Close approach perturbations with the migrating planets would destroy most binary systems which is contrary to observations (Parker & Kavelaars 2010).

In a not distant past, there have been good reasons to suppose that the CCKB was transported from inner regions of the primordial planetesimal disk by some mechanism associated with planetary migration (Levison & Morbidelli 2003; Levison et al. 2008). The reason for this was basically due to the fact that the CCKB has presently a very low mass estimated from  $3 \times 10^{-4} M_{\oplus}$

(Fraser et al. 2014) to 10 times as that number (Nesvorný et al. 2020). Classical planetesimal accretion theories would demand a fairly high initial mass in the CKB region in order to create objects as large as the real ones. Yet collisions among these objects are not efficient enough to grind them to the present CCKB mass during the Solar System age (Kenyon & Luu 1999). Moreover, a large mass in the primordial planetesimal disk would push Neptune to the outer border of the disk where the present KB is today (Gomes et al. 2004). More recently, however, new theories on planetesimal accretion, induced by streaming instability (Drażkowska & Dullemond 2014; Johansen et al. 2007; Youdin & Goodman 2005) (see also Morbidelli & Nesvorný (2020) for a review concerning the formation of the Kuiper Belt) can explain the formation of large planetesimals (100 km diameter) directly from cm-sized ice pebbles. The main idea behind these mechanisms is based on the radial drift of these pebbles rotating in a sub-keplerian regime due to drag induced by the disk gas. As the pebbles drift inwards, they accumulate into inner regions of the disk where the drift decreases or stalls due to too much mass in the pebbles that force the gas to rotate with the pebbles frequency. This on its turn provokes the accumulation of pebbles into certain regions of the disk which on its turn induces a gravitational instability that makes the pebbles to accumulate into a single large object. Streaming stability has been shown also to yield planetesimals in orbits that are compatible with the spatial orientation of Kuiper Belt binary orbits (Nesvorný et al. 2019).

A classical definition of the CCKB comes from its dynamical properties. According to that definition the CCKB is formed by objects in a certain semimajor axis range ( $\sim 42 - 47$  au) and inclinations below a certain value (usually  $4^\circ$  or  $5^\circ$ ). But CCKB objects also differ from the

rest of the TNOs by their physical properties of which their colors are probably the main characteristic. In fact, CCKB objects are mostly reddish, opposed to other TNOs whose color range from red to neutral colors. Another important particular characteristic of CCKB objects is that they usually appear in pairs, since most of them belong to a binary system. Nevertheless the binary TNOs inventory includes mostly cubewanos with very few scattering or detached objects, still fewer when we consider only similar size members binaries which are mostly associated to the CCKB objects.

With this in mind, I propose to define the Extended Cold Population (ECP)<sup>1</sup> as formed by objects in a certain range of color indices, like B-R. With this definition the orbital distribution of the ECP objects invades a larger region than that defined above based only in orbital characteristics. The idea is that the ECP is distinguished from the rest of the TNOs by the primordial region where it was formed and some primordial mechanism placed them not only on its classical KB region but some of them were transported to regions outside the CCKB. The main proposal in this paper is that the CCKB was not really formed in situ but experienced a short transportation process from the outermost part of the original planetesimal disk which would have an outer border somewhere around 42 au. My second proposal is that this assumption allows for the explanation of reddish objects outside the CCKB as well as the formation of the CCKB objects in a more massive environment than the present CCKB since although streaming instability theories may allow for the construction of large objects like those of

the CCKB, it is however questionable whether such a low mass as  $3 \times 10^{-4}$  to  $3 \times 10^{-3} m_{\oplus}$  can be formed within that theory.

This paper is divided as follows. In Section 2, I define the ECP that will serve as a reference to search for the best model to produce it. Section 3 describes the model used in this work. In Section 4, the main results are presented. Section 5 explains the mechanisms that were effective in generating the orbits associated to the ECP. In Section 6, I present some examples of numerical simulations including four or five planets and a disk of perturbing planetesimals in order to check for the viability of the proposed model. In Section 7, I discuss the results and present conclusions.

## 2. THE EXTENDED COLD POPULATION

As advanced in the Introduction, defining the cold population just by its orbit characteristics may not be the best approach. We might instead define the cold population by their colors or their binary feature. Of course, none of these possible definitions completely characterizes the cold population. But defining the cold population solely by its orbital characteristic can hide important information as to its origin. The inventory of discovered binary systems among the TNOs is not so large (in particular with respect to distant TNOs) as that of objects with defined color characteristics, thus I choose TNOs colors as a constraint to define the ECP.

In Johnston's archive website<sup>2</sup> one finds orbital elements of TNOs and their color characteristics, such as their B-R magnitude and their taxonomical color type (RR,IR,BR, etc.). I could define the ECP either by including in it all the objects belonging to the most reddish taxonomical types (RR or RR+IR) or by fixing a B-R magnitude above which all objects would belong to the ECP. To decide on the best choice,

<sup>1</sup> I keep the 'cold' adjective for this population's nomenclature to remind that all these objects share a common origin as that of the CCKB, acknowledging however that this extended population will include orbits with much higher orbital eccentricities and inclinations than those in the CCKB

<sup>2</sup> <http://www.johnstonsarchive.net/astro/tnoslist.html>

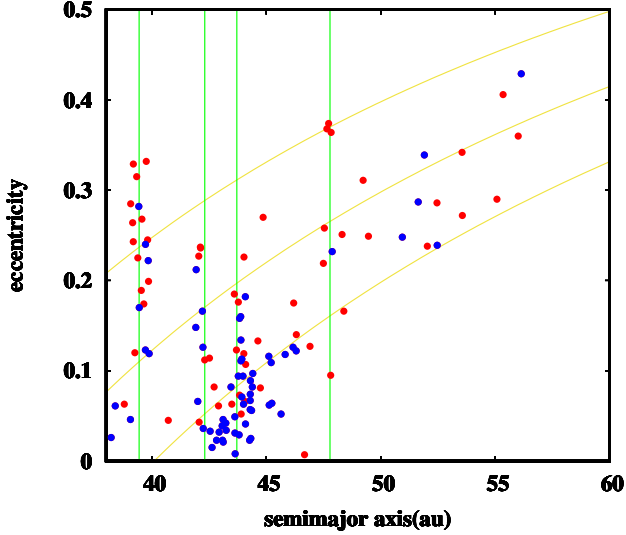


**Figure 1.** Distribution of semimajor axes and eccentricities of observed objects belonging to the ECP. Blue circles stand for objects with the orbital inclination  $I < 4^\circ$ . Otherwise they are represented by red circles

I separated a constrained part of the TNOs from the above table, defined by ranges in  $a$  (semimajor axes) and  $q$  (perihelion distances) given by  $42.5 \text{ au} < a < 46.5 \text{ au}$  and  $q > 38 \text{ au}$ , which will stand for the CCKB defined in this work. Then I computed the ratio of the number of objects that have their orbital inclination  $I < 4^\circ$  to the total number of objects in that subpopulation. This was done for objects associated to the RR type, the RR+IR type and those that have B-R magnitude greater than 1.58<sup>3</sup>. The largest ratio was obtained for the last subpopulation, the one defined by magnitude B-R  $> 1.58$ . This is a way of defining the ECP primarily by its color characteristics but somehow constrained by the fact that the CCKB is an important part of the total ECP and that it is composed mostly of low inclination objects.

<sup>3</sup> This magnitude was chosen based on a balance between yielding a high ratio of low eccentricity members to all others and keeping a reasonable number of objects in the ECP

Figure 1 shows the distribution of semimajor axes and eccentricities for objects that have their B-R magnitude larger than 1.58, taken from Johnston’s archive website. This will be defined as the observed ECP. To best compare with the results shown in following sections I further constrain the ECP just for objects with  $37 \text{ au} < a < 60 \text{ au}$ . I define three different subpopulations in the ECP: the CCKB, defined as objects with  $42.5 \text{ au} < a < 46.5 \text{ au}$  and  $q > 38 \text{ au}$ ; the distant cold population (DCP), defined by semimajor axes above the 2:1 MMR with Neptune ( $a > 49 \text{ au}$ ) and below 60au, this upper limit chosen since there are few objects with B-R magnitude greater than 1.58 and  $a > 60 \text{ au}$ ; the resonant population, defined for semi major axes around the nominal semi major axis for a specific MMR with Neptune. For the case of the resonances 5:3 and 7:4 objects with  $q > 38$  are considered belonging to the CCKB as stated above. For the 2:1 resonance I consider objects with their semimajor axes 1 au above or below the nominal resonant semimajor axis as belonging to the 2:1 resonance. Motivated by Fig. 1, I consider only the resonances 3:2, 5:3, 7:4 and 2:1. The DCP is specially revealing since it shows scattered / detached orbits with fairly low inclinations. Three of them, 2001 UR163, 1995 TL8 and 2002 GZ31, are still more conspicuous. They have semimajor axes in the range  $50.9 \text{ au} < a < 52.5 \text{ au}$ , perihelion distances in the range  $36.8 \text{ au} < q < 39.9 \text{ au}$  and inclinations below  $1.1^\circ$ . Far from important MMR with Neptune and with relatively low perihelia and low inclinations, their orbits are hardly explainable by classical mechanisms including resonance sticking followed by the coupling of MMR with Neptune with Kozai resonance (Brasil et al. 2014b,a; Gomes 2011).

### 3. THE MODEL

The simulations undertaken for this work were initially motivated aiming at creating a transportation mechanism that would preserve the

planetesimals’ eccentricity. Although a local origin for the CCKB is widely accepted as the best explanation for the present orbital distribution of the CCKB objects, it may however be difficult to accommodate a local formation scenario that can account for both the CCKB and the rest of the ECP, in particular the DCP. Transporting mechanisms for the CCKB have failed mostly because they yielded too excited orbits for the CCKB objects (Levison et al. 2008; Levison & Morbidelli 2003). This is basically due to the eccentricity excitation as an effect of the resonance sweeping mechanism to transport planetesimals from inner regions of the planetesimal disk (Malhotra 1995; Gomes 1997). A way out to avoid this eccentricity excitation in a resonance sweeping scenario is to consider corotation resonances instead of libration resonances (Ward & Canup 2006). In order to accomplish that one must consider an eccentric perturbing body, in our case Neptune. Thus I consider a scenario based on the classical Nice model (Tsiganis et al. 2005; Gomes et al. 2005, 2018) in which the planets, including Neptune, acquire fairly excited orbits during their close encounter phase. In this scenario, at some point in the planetary orbital evolutions, the close encounters phase comes to an end and the planets experience a residual migration with a circularization of their orbits. In the simulations here presented I assume that the planets have just ended their mutual close encounters phase (or are about to end) and start their final evolution to their current orbits due to the remaining perturbing planetesimals. In Section 6 I present some results of numerical integrations of planets and massive planetesimals that may give some indication of what kind of disk may be consistent with the assumptions here made for the final phase of planetary migration represented by the synthetic model. In this manner I consider the semimajor axes for the giant planets as  $a_N = 25$  au,  $a_U = 17$  au,  $a_S = 9.35$  au

and  $a_J = 5.2$  au. Jupiter is considered in its present orbits since it migrates much less than the other giant planets and its small migration will have roughly no influence in the mechanisms presented in this work. Uranus and Saturn initial semimajor axes are based on mean ratios of their semimajor axes variations to Neptune’s obtained in numerical integrations with a massive planetesimal disk (Gomes et al. 2018). The initial eccentricities of Neptune and Uranus are respectively 0.3 and 0, chosen so as to make them near but not in a close encounter regime. Other orbital elements were chosen as the current ones, except for Neptune’s mean longitude which was chosen randomly from  $0^\circ$  to  $360^\circ$ . Neptune’s mean longitude is the only orbital element that will be different for each integration and its random choice will be sufficient to yield quite different evolutions for the integrations. The null eccentricity for Uranus is just a trick to start integrations in order to yield more effective results, in order to avoid deep close encounters between the ice planets from the beginning which may cause the ejection of one of the ice planets. Although artificial, it is not an unrealistic supposition since in planetary instability migration models Uranus and Neptune experience expressive oscillations of their eccentricities and either of them may be temporarily quite low, what the synthetic model in fact reproduces since Uranus eccentricity is immediately raised by Neptune’s high eccentricity. From those initial conditions I start numerical integrations of the four giant planets including a synthetic force on Neptune and Uranus to account for the residual migration and circularization of their orbits. This force is constructed by applying the following accelerations on the planets.

$$A = K \exp -t/\tau (1 + C \cos \lambda) \quad (1)$$

where  $A$  is the absolute value of an acceleration applied in the direction of the planet’s velocity,



$K$ ,  $\tau$  and  $C$  are constants and  $\lambda$  is the planet's mean longitude. The constant  $K$  is defined by  $\tau$  and the initial ( $a_i$ ) and final ( $a_f$ ) semimajor axis of the planet through:

$$K = -\frac{GM}{\tau} \left( \frac{1}{a_f} - \frac{1}{a_i} \right) \quad (2)$$

where  $G$  is the gravitational constant and  $M$  is the Sun's mass.  $\tau$  is the timescale of the exponential semimajor axis evolution and the constant  $C$  controls the variation of the planet's eccentricity. The values of  $\tau$  and  $C$  were chosen to mimic the evolution of the planets' semimajor axes and eccentricities just after the close encounter phase, as observed in some numerical integration done for previous works (Gomes et al. 2018). They are  $\tau = 1.37My$  and  $C = -15$  for most of the planetary evolution. In the beginning (up to 1.4 My) I use a smaller (in absolute value)  $C = -2$  to account for a time when Neptune still keeps a moderately high eccentricity and guides the resonance sweeping. When Neptune's eccentricity is lower than 0.1 I also use a damping variation of  $C$  to account for a smooth circularization of the planet's orbit. This is given by:

$$C = C_0 (e_P/0.1)^2 \quad (3)$$

where  $e_P$  is the planet's eccentricity and  $C_0$  is the old value of  $C = -15$ .

The planetesimals are considered massless in the outer border of a planetesimal disk. I consider this outer part of the disk from  $a = 39.5$  au to 42.5 au and refer to it hereafter as the Outer Border Disk (OBD). Semimajor axes for the planetesimals are chosen uniformly on that range. The eccentricities are chosen randomly in the range 0 to 0.05 and the inclinations also randomly from  $0^\circ$  to  $1^\circ$  with respect to the invariant plane. The eccentricities and inclinations are chosen in a somewhat ad-hoc manner but aiming at giving a small excitation due to an expected moderate past perturbation by

the excited planets during their close encounters phase. It is important to note that in many cases of numerical integrations with planets and a massive planetesimal disk the position from where Neptune starts its final free-of-encounters migration is attained quite abruptly from a smaller semimajor axis that would only slightly perturb the OBD. Other orbital elements were chosen randomly from  $0^\circ$  to  $360^\circ$ . The OBD is supposed to be the outermost part of the planetesimal disk. The OBD's total mass can be approximated to zero in the simulations since it is supposed to perturb the planets in a negligible manner. We also assume that whatever the planetary dynamics during the close encounter phase was, it did not greatly disturb the OBD. The inner portion of the disk (below 39.5 au) is not here considered and is supposed to have influenced the dynamics of the planets during the close encounters phase and must be mostly responsible to form the hot population although some of the outermost part of this inner portion may also partially contribute to the ECP. The inner border of the OBD at 39.5 au was chosen in order to associate it to Neptune's initial semimajor axis at 25 au which yields the 2:1 MMR with that planet at  $\sim 39.7$  au.

The choice of random orbital longitudes for Neptune's initial orbit yields sufficient randomness to the evolution of the pair of ice planets. So although Neptune and Uranus are initially in non-crossing orbits, in many cases they attain close encounter orbits in the beginning of their evolution. Some of these evolutions end with one of the ice planets being ejected from the solar system. Moreover the final semimajor axes of Uranus and Neptune can differ from their real actual ones from up to 2 au. This is expected since the synthetic accelerations were constructed based on a non perturbed orbit. Since I am interested in the final orbital distribution of the planetesimals started in the OBD when the planets have their current semimajor

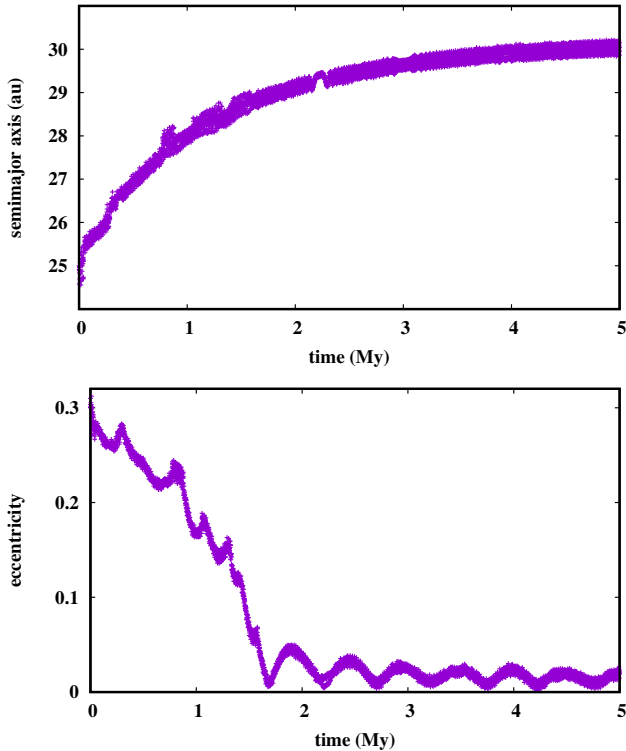


**Figure 2.** Evolution of Neptune’s semimajor axis and eccentricity for one of the simulations based on the synthetic model

axes, either (1), in the case Neptune stops before 30.1 au, I stretch the integration for another 1 My applying synthetic accelerations on Uranus and Neptune so that they migrate linearly (here with no influence in the eccentricities) and stop at their current semimajor axes, or (2), in the case Neptune stops past 30.1 au, I consider the orbital distribution of planetesimals at the time when Neptune’s mean semimajor axis was at 30.1 au. Figure 2 shows an example of the evolution of Neptune’s semimajor axis and eccentricity for one of the integrations.

#### 4. MAIN RESULTS

The final distribution of the planetesimals initially at the OBD is finely dependent on the particular evolution of the ice planets, particularly on Neptune, whereas the planets evolution is finely dependent on the initial mean longitude of Neptune. In general the planetesimals park

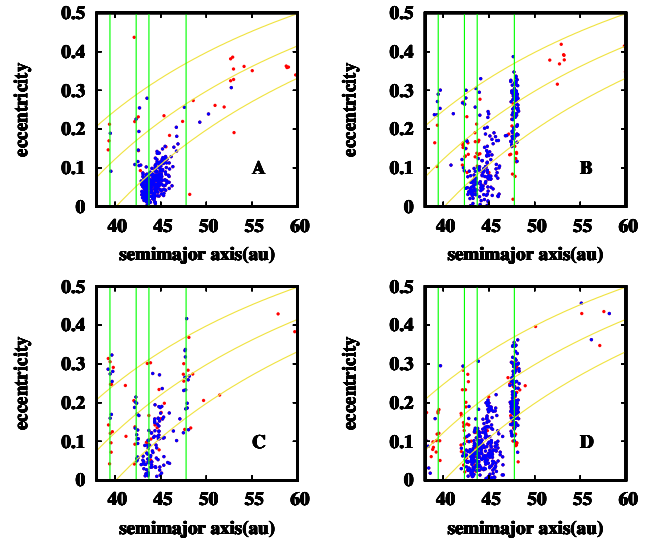


**Figure 3.** Distribution of semimajor axes and eccentricities of planetesimals transported to the CCKB from four different simulations. Inclinations lower than  $4^\circ$  are represented by blue dots, otherwise red dots. The vertical lines stand for the MMRs with Neptune, respectively, from left to right, the 3:2, 5:3, 7:4 and 2:1. The curved lines define constant perihelion distances  $q = 30$  au,  $q = 35$  au and  $q = 40$  au.

at three main regions: (1) the CCKB, (2) the DCP and (3) in MMRs with Neptune, mostly the 2:1, 3:2, 5:3 and 7:4. It can be quite hard to select the best orbital distribution of the ECP obtained by the simulations by comparing it to the real objects’ orbital distribution belonging to the ECP as defined by their colors and shown in Fig. 1. One would have to compare distributions of semimajor axes, eccentricity and inclination in the CCKB, ratio of number of objects in the resonances and the DCP to those in the CCKB, etc. I chose to only compare (1) the semimajor axis distribution in the CCKB, the ratio of the number of objects in the DCP to the number of objects in the CCKB and the ratio of the number of objects in the 2:1 MMR with Neptune to those on the CCKB. More detailed comparisons would complicate too much a problem that is particularly influenced by observational bias. It must be noted that the num-

ber of reddish objects in each of the considered subpopulations is influenced by the desire of the observer to obtain the photometry of that particular object and this is an important source of bias. After submitting the final results to the above mild constraints I also submitted them to visual inspections and the best of them were chosen to have their evolution continued to 4.5 Gy. Four of these case are shown in Fig 3.

Although none of the four cases shows a perfect comparison with the real data all of them show objects in all subpopulations (CCKB, DCP and MMRs with Neptune). The very specific orbital distribution of the ECP is finely dependent on the orbital evolutions of the giant planets and more specifically on Neptune.

The number of planetesimals implanted in the CCKB is just a fraction of those initially in the OBD. The cases depicted in Fig. 3 are associated to a fraction of the OBD deposited in the CCKB ranging from 1 to 5%. From a total mass in the CCKB estimated at  $3 \times 10^{-4} M_{\oplus}$  (Fraser et al. 2014) to 10 times as that (Nesvorny et al. 2020) we can reckon a mass in the OBD ranging from  $0.006 M_{\oplus}$  to  $0.3 M_{\oplus}$ . This larger mass may be more compatible for the formation of the CCKB objects from streaming instability scenarios that form a relatively larger total mass in CCKB objects. On the other hand, the largest mass estimated for the OBD ( $0.3 M_{\oplus}$ ) if extended to 30 au with the same density as for the OBD would entail a total mass beyond 30 au of around  $1 M_{\oplus}$  which would not be high enough to bring Neptune to the edge of the planetesimal disk (Gomes et al. 2004). Even for a density of the disk beyond 30 au to the inner edge of the OBD around five times as large as the density at the OBD, which would imply a total of  $5 M_{\oplus}$  beyond 30 au, Neptune would hardly migrate farther than 30 au. In Section 6, I present results from numerical integrations of the primordial planets and a disk

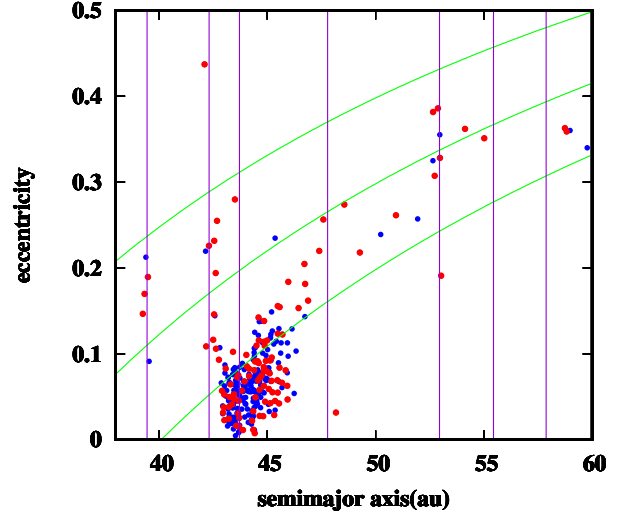


**Figure 4.** Distribution of semimajor axes and eccentricities for the case in panel A of Fig. 3 when, like Fig. 3, the outer border of the OBD is at 42.5 au (blue circles) and for the outer border at 41.5 au (red circles) Vertical lines stand for the nominal position of the main MMRs with Neptune, from left to right the 3:2, 5:3, 7:4, 2:1, 5:2, 8:3 and 3:1. The curved lines define constant perihelion distances  $q = 30$  au,  $q = 35$  au and  $q = 40$  au.

of massive planetesimals where this question is farther discussed.

The outer border of the OBD was chosen in a somewhat ad-hoc manner, only making sure that all particles in the OBD would be transported. But it may not be necessary that the disk border is exactly at 42.5 au. With the results here obtained we can check for other possible outer borders for the OBD, just excluding the planetesimals that had their semimajor axes above a given value from the final results. In the examples considered here there is not much difference in the final distribution of planetesimals in the ECP when we consider a lower border for the OBD. A typical example can be noticed in Fig. 4 where I plot again the distribution of planetesimals in the ECP for the case of panel A of Fig. 3 in the case with the disk border at 42.5 au (blue) and at 41.5 au (red). In this figure, the number of red dots is 136 and the total number of particles is 328, which correspond



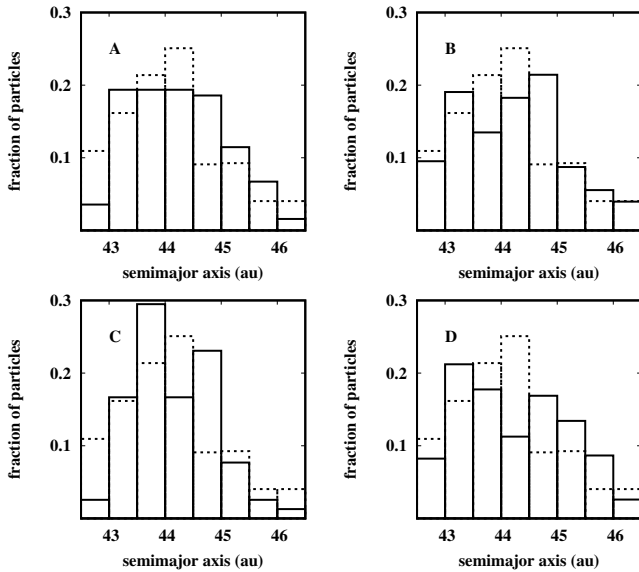


**Figure 5.** Histograms of the distribution of semimajor axes for the same simulations as those depicted in Fig. 3. The dashed lines stand for the real case

to fractions of implanted planetesimals from the shorter and longer OBD (with respectively 3333 and 5000 planetesimals) respectively 0.041 and 0.066. The fraction of planetesimals implanted in the ECB from the OBD is usually smaller for an OBD outer border at 41.5 than at 42.5.

Figure 5 shows the histograms of semimajor axes of all planetesimals implanted in the CCKB from the results depicted in Fig. 3, in which the labels A-D correspond to the same case as in Fig. 3. In dashed line, the histogram for the real CCKB is presented for comparison. Again, although in no case there is a perfect agreement, we can conjecture that the real distribution of CCKB objects are due to a very specific Neptune’s evolution. On the other hand, we can see that there is always a bin of semimajor axes for any case (except maybe for case A) in which there is a maximum in the number of planetesimals.

## 5. TRANSPORTING MECHANISMS TO THE ECP

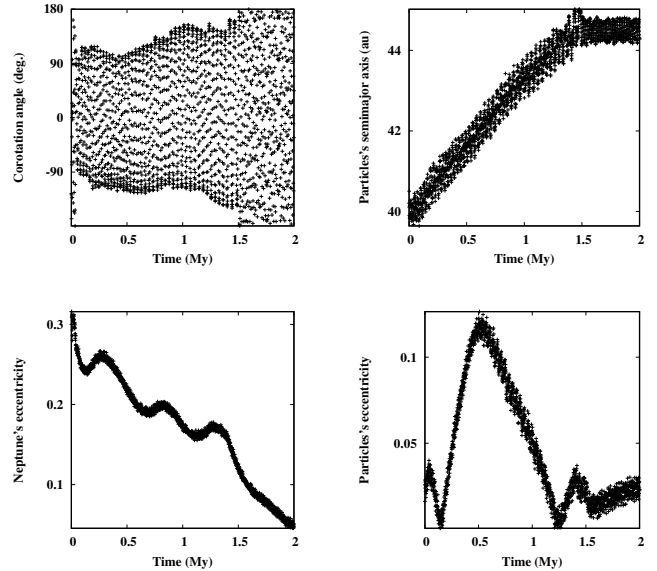


**Figure 6.** Example of the evolution of orbital elements of a planetesimal initially trapped in the 2:1 corotation MMR with Neptune and released from the resonance at the CCKB

I consider separately in the following subsections the transporting mechanisms for three distinct subpopulations of the ECP, the CCKB, the DCP and the resonant population.

### 5.1. The CCKB

This is the most important part of the ECP. The main mechanism responsible for the formation of the CCKB is commented in Section 3 as the motivating reason for this work. An eccentric Neptune captures planetesimals into its 2:1 corotation resonance. When this planet migrates it conveys planetesimals outwards with it and when Neptune’s orbit is around 28 au and fairly circular several planetesimals are released from the resonance and implanted in the CCKB region around 44 au. Of course, the final distribution of orbits in the CCKB is quite sensitive to the very peculiar evolution of Neptune’s orbit, as depicted in Fig. 3. A typical evolution of a planetesimal that experiences the main mechanism that conveys planetesimals to the CCKB is shown in Fig. 6. The planetesimal is captured into the 2:1 corotation resonance

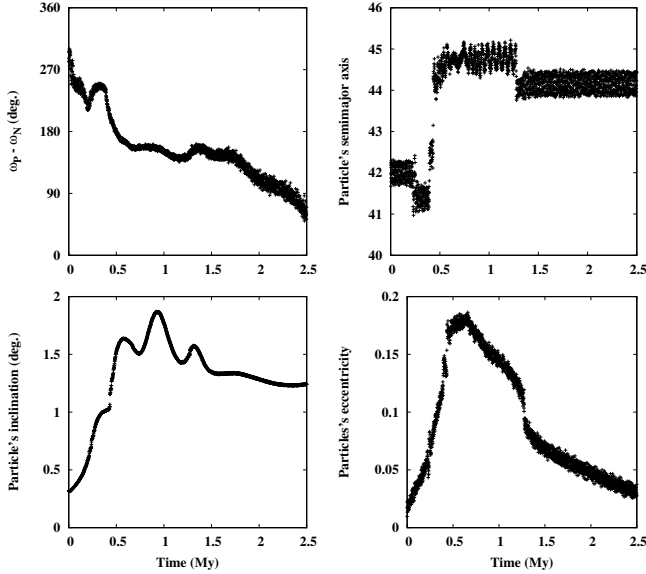


**Figure 7.** Example of the evolution of orbital elements of a planetesimal that was scattered by Neptune and eventually deposited in the CCKB

with Neptune at the beginning of its evolution, as indicated by the evolution of the corotation angle ( $2\lambda_P - \lambda_N - \varpi_N$ ). At some point, when Neptune’s eccentricity is around 0.12 the resonance is broken and the particle is parked with  $a \sim 44.2$  au and  $e \sim 0.03$ . It is noteworthy that, contrary to the libration resonance evolution, in which the planetesimal’s eccentricity experience a monotonic increase, in the corotation case, there may be eccentricity increases due to Neptune’s own high eccentricity but it is not monotonic. It shows an oscillatory variation and at the point of resonance break the eccentricity can be low enough as expected for a member of the CCKB. Inclination evolutions are not shown. They are kept always low as expected. They mostly reflect their initial values. During this kind of planetesimal evolution there is never a close encounter between it and Neptune, as expected, preserving in this manner the binary feature of the CCKB objects.

Yet, there is another mechanism that was found to occur in several cases of planetesimals deposited in the CCKB. Fig. 7 depicts a typical such case. It is like the typical case of planetes-

imals transported to the DCP and more details of this mechanism will be explained in Section 5.2. But the complete mechanism includes a fast semimajor axis variation due to close encounter perturbations with Neptune, an escape from this regime as Neptune’s eccentricity decreases followed by a decrease of the particles’ eccentricity which will be explained with more detail in the following subsection. In most integrations that yielded a nice CCKB distribution at the end of the migration phase, the prevailing mechanism is the former one explained above. But the latter one also appears with non negligible frequency and in some integrations it can reach about 30% of the cases. The problem with this mechanism is that it is expected to destroy the binary feature of the CCKB objects by coming too close to Neptune (Parker & Kavelaars 2010). But contrary to one’s expectation this is not quite true. For the cases depicted in Fig. 3 I redid the integrations computing at every integration step the distance of each planetesimal to Neptune and I output this distance and the time whenever a planetesimal was less than 2 au far from Neptune. In the example shown in Fig. 7, I found that the distance of the planetesimal to Neptune was never smaller than 2 au. Fig. 8 shows the distribution of semimajor axes and eccentricities for the cases in panel A and B of Fig. 3, showing only the CCKB and highlighting the planetesimals that got closer than 2 au from Neptune by a larger black circle. Case B (lower panel) is the one with more instances of close encounters. For this case, there are 19 planetesimals in 126 (thus  $\sim 15\%$ ) that got closer than 2 au from Neptune during their evolutions, all of them for less than 2 Ky. For the same case, 10 planetesimals got closer than 1 au, all of them for less than 210 years during their evolutions. Although a detailed analysis of the evolution of CCKB-like binary systems perturbed by Neptune during the evolutions here described is out of my scope, the distances of

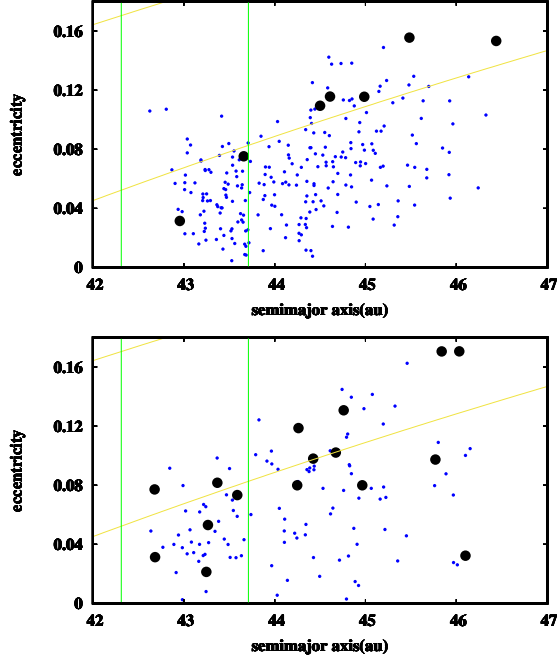


**Figure 8.** Two examples of the distribution of semimajor axes and eccentricities coming from panel A of Fig. 3 (upper panel) and panel B of Fig. 3 (lower panel) where planetesimals that were at some time closer than 2 au from Neptune are represented by large black circles

the planetesimals to Neptune above calculated suggest with good confidence that most objects transported to the CCKB will preserve their binary feature.

### 5.2. The Distant Cold Population

The second mechanism for transporting planetesimals to the CCKB is the one responsible to fill the DCP region. Figure 9 shows the evolution of orbital elements of a typical case. The typical behavior includes three main phases: (1) by the effect of an eccentric Neptune, the planetesimal’s eccentricity increases until (2) a phase of close encounters with Neptune starts when the planetesimal’s semimajor axis increases until (3) by Neptune’s eccentricity decrease the close encounter phase ceases and the planetesimal’s eccentricity decreases to a safe value that corresponds to a stable orbit for the planetesimal. The phase of poten-

tial close encounters is delimited by two vertical lines, where  $d < 0$ . What deserves an explanation is the planetesimal’s eccentricity decrease after the close encounter phase. This is due to a still strong secular influence of a still nearby Neptune on the planetesimal and the fact that  $\varpi_P - \varpi_N$  is in the right phase to yield the planetesimal’s eccentricity decrease, which can be seen in the left-upper panel of Fig. 9. In fact, to its lowest order, the secular variation of the planetesimal’s eccentricity is given by:

$$\dot{e} = -\frac{1}{na^2e} \frac{dR}{d\varpi} \quad (4)$$

$$R = -\frac{1}{4} G m L e e_N \cos(\varpi - \varpi_N) \quad (5)$$

where  $n$ ,  $a$ ,  $e$  and  $\varpi$  are respectively the mean motion, semimajor axis, eccentricity and longitude of the perihelion. The index  $N$  stands for Neptune whereas no index stands for the planetesimal.  $R$  is the disturbing function,  $G$  is the gravitational constant,  $m$  is Neptune’s mass and  $L$  a Laplace coefficient depending on the semimajor axes of the planetesimal and Neptune. Thus we can write:

$$\dot{e} = -C_+ \sin(\varpi - \varpi_N) \quad (6)$$

where  $C_+ = (G m L e_N)/(4 n a^2)$  is a positive constant (depending on  $e_N$ ). Thus when  $\varpi - \varpi_N$  is between  $0^\circ$  and  $180^\circ$ ,  $\dot{e} < 0$ . Moreover just after the close encounter phase when  $e_N$  is still large, the effect on  $\dot{e}$  is likewise large.

Figure 10 shows the variation of  $\varpi_P - \varpi_N$ , where the index  $P$  stands for a planetesimal,  $q_P$  and  $q_P - Q_N$ , where  $q_P$  is the perihelion of the planetesimal and  $Q_N$  is Neptune’s aphelion. They refer to planetesimals that parked in the DCP at 10 My from the integration depicted in panel A of Fig. 3. It can be noticed that the perihelia of these planetesimals experience an increase during the time  $\varpi_P - \varpi_N$  is in the right range. Of course after a planetesimal is

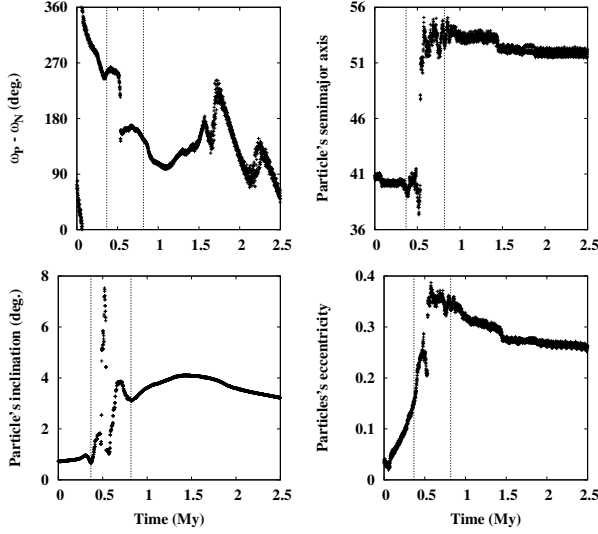


**Figure 9.** Evolution of orbital elements of a planetesimal that was implanted in the DCP

free from close encounters with Neptune, the behavior of its eccentricity will depend on the specific phase of  $\varpi_P - \varpi_N$  and those that are in the right phase to have their eccentricity decreased are just a fraction of all that were scattered by Neptune. Fig. 11 shows the continuation of the evolution of  $\varpi_P - \varpi_N$  and the eccentricity of the same planetesimal as that of Fig. 9. When the planetesimal and Neptune are far enough  $\varpi_P - \varpi_N$  circulates faster and the eccentricity starts a periodic variation around its relatively low eccentricity.

Now some words are in order about the close encounter history of the DCP planetesimals as formed by the above mechanism. Figure 12 shows a histogram of smallest close encounter distances from Neptune of the planetesimals that became a member of the DCP at 3 Gy, from the run depicted in panel A of Fig 3. This can be compared with Fig. 2 of Parker & Kavelaars (2010). Studying the final effect on putative binaries of the encounters that preceded the implantation of these objects into the DCP is out of the scope of this work. On the other hand, the inventory of binary TNOs with semi-major axis in the range 50 au to 60 au and that have their B-R magnitude measured as greater

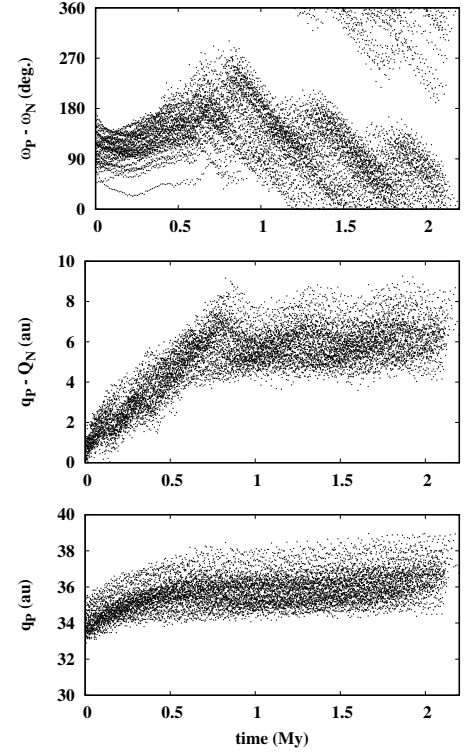


**Figure 10.** Evolution of the orbital elements of several planetesimals that were implanted in the DCP: planetesimals' perihelia, the difference of planetesimals' perihelia to Neptune's aphelion and the difference of planetesimals' longitudes of the perihelion to Neptune's longitude of the perihelion.

than 1.58 is still small for an accurate statistics. Moreover whatever the mechanisms that were responsible for the implantation of red objects into the scattered / detached population, it is expected that these mechanisms included episodes of close encounters with Neptune, thus one should not expect the preservation of binary systems as a rule.

### 5.3. The Resonant Population

The mechanism which is the easiest to explain the filling of a resonant region with ECP objects is that associated with the 2:1 resonance. Figure 13 shows a typical case. The peculiar behavior in this case is depicted by the evolution of the 2:1 resonant angle, in which the active resonant angle alternates from a corotation to a libration and this change occurs at about

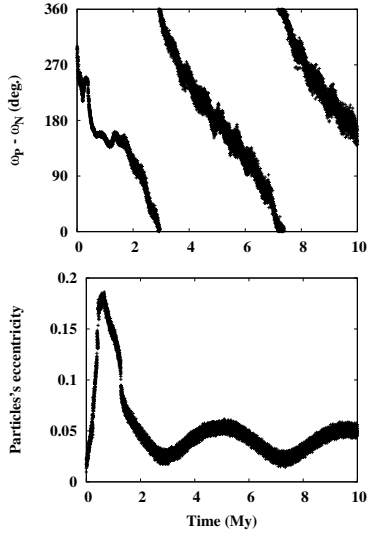


**Figure 11.** Continuation to 10 My of the evolution of the eccentricity and the difference of the planetesimal’s longitude of the perihelion to Neptune’s, for the same case as in Fig. 9

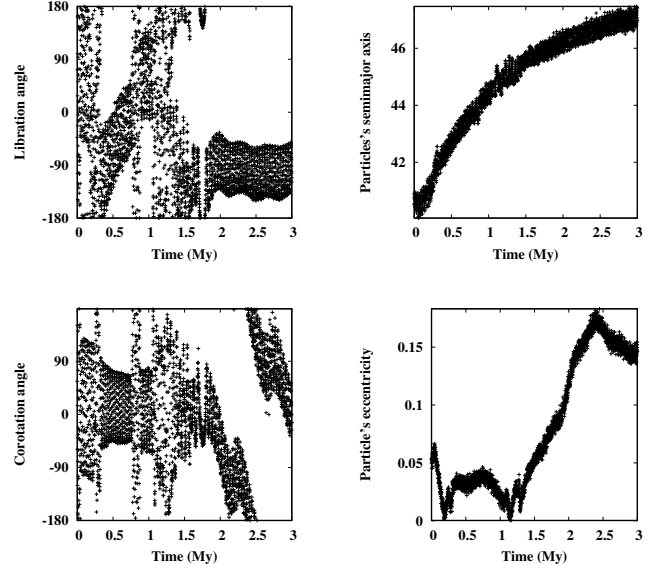


**Figure 13.** Evolution of orbital elements of a planetesimal that was trapped in the 2:1 MMR with Neptune

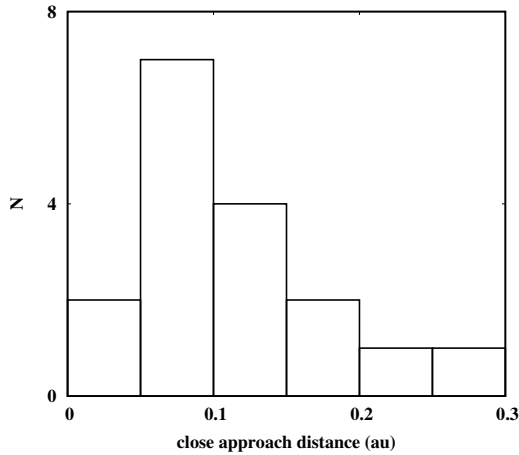


**Figure 12.** histogram of smallest close encounter distances from Neptune of the planetesimals that became a member of the DCP at 10 My, from the run depicted in panel A of Fig 3

1.7 My. This example is didactic since it shows that the corotation and libration resonances are not well separated. While the corotation resonance is active, the libration angle shows a kind of libration with a varying libration center, whereas after 1.7 My the opposite is true. This is associated to the fact that  $\varpi_P - \varpi_N$  has a relatively slow variation and this on the other

hand is likely what drives the specific variation of the particle’s eccentricity while in corotation resonance with Neptune. The total number of planetesimals trapped into the 2:1 MMR with Neptune as well as the ratio of this number to the number of planetesimals implanted in the CCKB depends sensitively on the very final evolution of Neptune as suggested by Fig. 3. Thus the evolution depicted in Fig. 13 suggests that understanding the process by which planetesimals are either released in the CCKB or switch from corotation to libration resonance is fundamental to possibly constrain this final evolution of Neptune so as to produce the actual relative distribution of planetesimals in the CCKB and the 2:1 MMR. The eccentricities attained by the planetesimals in the 2:1 MMR with Neptune by the proposed mechanism, which is approximately between 0.15 and 0.3, implies an original trapping by Neptune into the libration resonance when the planetesimals are between 42 au and 44 au with eccentricities from 0 to 0.1 considering their monotonic variation induced by the exchange of angular momentum and energy



with the migrating Neptune by which the planetesimals are being swept in resonance (Gomes 1997).

The other important resonances with Neptune are the 3:2, 5:3 and 7:4. As for these last two, the trapping into these resonances usually occurs as a secondary process after the planetesimal has been transported some way out by the same process that creates the CCKB. As for the 3:2 resonance, there is always a close encounter with Neptune and the planetesimal eventually enters the 3:2 resonance from a scattering orbit by a resonance sticking mechanism. In some cases, there is a residual migration associated with Neptune’s residual migration. The 3:2 resonance is the less typical according to the scenario proposed in this work. It does not mean that it will be less populated by ECP particles since I chose 39.5 au as the inner border of the OBD in order to explain the formation of the CCKB and DCP. There must be other reddish particles originally with  $a < 39.5$  and some of these must be affected by the 3:2 resonance with a migrating Neptune. But then this process will depend significantly on the very specific evolution of Neptune before the assumed beginning used in the simulations here presented. This scenario that can produce Plutinos would need another approach which is beyond the scope of this work.

## 6. DOES THE SYNTHETIC MODEL HAVE A REAL COUNTERPART?

The model presented in Section 3 was constructed aiming at a specific result, bringing the outermost part of the primordial disk of planetesimals to fill the present CCKB and the rest of the ECP. A fair question that imposes is: Can real evolutions of the present giant planets (and possibly other cores that were ejected from the Solar System) migrating in a planetesimal disk yield the conditions for Neptune to experience the specific evolution presented in Section 3 that can spread the original OBD onto the

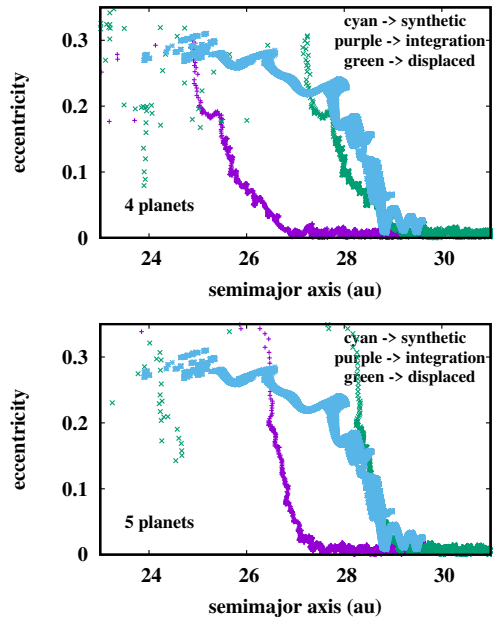


**Figure 14.** Comparison of the evolution of Neptune’s semimajor axis and eccentricity for the synthetic case that generated the example of panel A in Fig. 3 with Neptune’s orbital elements from two numerical simulations of the planets in a massive planetesimal disk, one case with four planets and another one with five planets. Neptune’s orbital elements are with respect to the barycenter of the system including the Sun and the other three planets inside Neptune’s orbit.

ECB? In order to answer this question I did several numerical integrations of the giant planets perturbed by a planetesimal disk. I considered both a four-planets model and a five-planets model (Nesvorný 2011; Nesvorný & Morbidelli 2012). Table 1 gives the initial orbital elements of the planets. The planetesimal disk for the 4-planets model was considered with a total mass chosen randomly for each integration between  $25M_{\oplus}$  to  $40M_{\oplus}$ , an inner border at 13 au and an outer border at 35 au, and for the 5-planets model, the mass was  $25M_{\oplus}$  to  $35M_{\oplus}$ , the inner border at 17 au and the outer border also at 35 au. These conditions were chosen based on previous integrations (Gomes et al. 2018) aiming at parking the planets near their present orbits but also aiming at allowing Neptune to

**Table 1.** Initial orbital elements for the planets

Planet	semi-major axis (au)	eccentricity	inclination (deg.)
5-Planets Model			
Jupiter	5.60141	0.02357	0.02627
Saturn	7.32016	0.08123	0.06867
Core1	10.28600	0.11279	0.11508
Core2	12.29610	0.06361	0.06063
Core3	16.56300	0.02534	0.04085
4-Planets Model			
Jupiter	5.41097	0.04089	0.05080
Saturn	8.63125	0.01907	0.05676
Core1	11.30040	0.03608	0.09070
Core2	14.93020	0.00629	0.03500

experience a final evolution similar to that presented in Section 3. In this respect stretching the disk to 35 au is important in order to allow Neptune to have its eccentricity decreased along with a small but non negligible semimajor axis increase. For this to be accomplished when Neptune is eccentric its aphelion must invade a planetesimal populated region otherwise the orbital circularization will not concomitantly be followed by a semimajor axis increase.

Figure 14 shows the variation of the semimajor axis with the eccentricity of Neptune for two cases, one from the 4-planets model and the other one for the 5-planets model. In both cases they are compared to a synthetic evolution on Neptune, the one associated with panel A of Fig. 3. In both cases I also plot the numerical integration case displaced in semimajor axis so as to superimpose it to the synthetic model. This is just an artifice to better show that the variation of semimajor axis and eccentricity imposed by the synthetic model has a real counterpart except possibly for the position of Neptune when its final decrease of eccentricity takes place. This behavior occurs for both models but is more frequent for the 4-planets

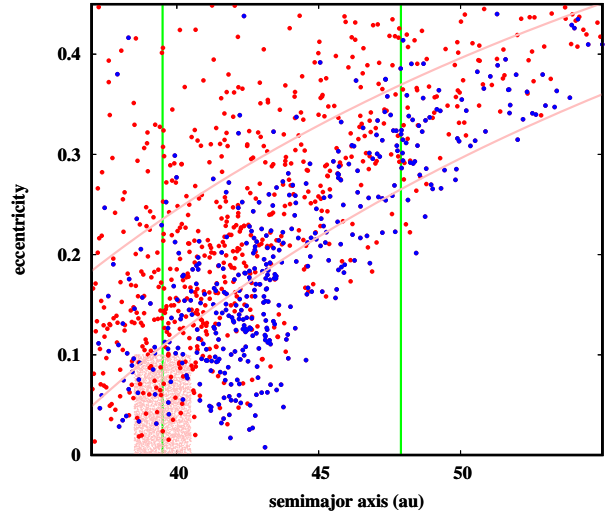


**Figure 15.** Initial (pink dots) and final semimajor axis and eccentricities distribution of planetesimals in an outer border disk that was perturbed by the planets in the numerical simulation with five planets as depicted in Fig. 14, lower panel. Blue circles stand for inclinations below  $5^\circ$  and red circles otherwise. Vertical lines stand for the position of the 3:2 and 2:1 resonance with Neptune. Other lines stand for the semimajor axes and eccentricities that yield  $q = a_N$  and  $q = a_N + 5$  au.

one. This is possibly caused by the fact that the initial semimajor axis for the outermost planet in the 4-planets model is not so far as for the 5-

planets model. This makes us guess whether a 6-planets model might give still better results in this sense. This is a way to shift the outermost planet farther outwards and keep the planets close enough to trigger a planetary instability scenario that can yield an eccentric enough Neptune which is required for the present model. An investigation of a six-planets model can be useful to check for that possibility and and this is planned as a future work.

With the initial orbital elements as shown in Table 1 and the disk masses as indicated above, Neptune’s average semimajor axis at the end of the integrations at 50 My was 26.7 au and 28.6 au, respectively for the 4-planets and the 5-planets model. Allowing for 1–2 au extra migration for Neptune at 4.5 Gy (based on some integrations that were extended to 4.5 Gy) we can estimate that the mass chosen for the planetesimal disk was reasonable so as not to let Neptune migrate too far (Gomes et al. 2004). The planetesimal disks extension and mass entail a total mass beyond  $30au$  (and to 35 au) between  $6.9M_{\oplus}$  and  $9.6M_{\oplus}$  which seems consistent with the estimated mass in the OBD of  $0.3M_{\oplus}$  at most, as indicated in Section 4. It must be noted that migration models that yield eccentric planetary orbits produce final semimajor axis for Neptune systematically smaller than for the case of models where Neptune sweeps a cold planetesimal disk.

Figure 15 shows the distribution of semimajor axes and eccentricities of massless particles started with the semimajor axis and eccentricities depicted in the same figure with pink dots. These initial conditions for the planetesimals represent an OBD displaced inward with respect to that considered in the synthetic simulations since, as shown in Fig. 14 lower panel, Neptune’s eccentricity decrease starts from a lower semimajor axis as compared to the synthetic simulations. Larger dots stand for the same particles at 50 My of the numerical integration

including the perturbing planets that evolved according to the 5-planets numerical simulation that yielded Neptune’s semimajor axis and eccentricity evolutions as shown in the bottom panel of Fig. 14. Blue dots stand for particles with the inclination  $I < 5^{\circ}$  and red dots otherwise. Although in several aspects different from the real distribution of the ECP, this figure however shows the main characteristics of the formation of the ECP: a CCKB between the 3:2 and 2:1 MMR with Neptune, the DCP beyond the 2:1 resonance and a few particles at the 2:1 MMR with Neptune. The main difference is in the location of the CCKB which is shifted towards the 3:2 MMR with Neptune and consequently farther from the 2:1 MMR. It is also transported on a smaller range from the initial OBD as compared to the results from the synthetic model. There is also an excess of dynamically hot particles, but this can be blamed at the small time span for which the integration was developed. Most high eccentricity particles must be shifted out of the CCKB after 4.5 Gy. A nice result shown by this figure is the formation of low inclination, high perihelion DCP particles, a result in better accordance with the real observed DCP than the DCP obtained by the synthetic model. The shortcomings described above with respect to the position of the CCKB comes from the fact that Neptune’s decrease in eccentricity occurs at lower semimajor axis and there is a longer residual migration of Neptune. More simulations can be done to check for the possibility of a better evolution of Neptune, including a 6-planets model.

## 7. DISCUSSION AND CONCLUSIONS

Cold Classical Kuiper Belt objects are today consensually considered as having an in situ formation. It is also consensus that CCKB objects have a specific physical characteristic evidenced by their reddish colors. This particular feature claims for the need of a common origin for all reddish TNOs which argues for a mech-

anism that may both implant the CCKB in its present location but also other reddish objects (Extended Cold Population) on their present locations. This fact motivated the present work in which an alternative scenario for the appearance of the Cold Classical Kuiper Belt is presented. In this scenario, the objects pertaining to the CCKB were transported a short range from the outer border of a primordial planetesimal disk. The same mechanism that implanted the CCKB on its present location would also be responsible for the implantation of objects with similar color characteristics as scattered / detached objects with moderately low inclinations. The mechanism is based on a classical Nice model in which Neptune acquires a high eccentricity and experiences a simultaneous orbital circularization and residual migration that are responsible to moderately convey the outer planetesimal disk outwards, keeping their relatively low eccentricities and low inclinations. The planetesimals are transported by a 2:1 corotation resonance sweeping process with Neptune and the planetesimals' implantation is accomplished by the eventual decrease of Neptune's eccentricity and the planetesimals release from the resonance.

An important byproduct of this mechanism is the formation of a relatively low inclination population of scattered and detached objects beyond but not far from the 2:1 MMR with Neptune. There are real objects occupying that region and they are not easily if at all explainable by a local formation of the CCKB. In fact, the mechanism here presented requires an episode of an eccentric Neptune as opposed to a scenario where Neptune is never or just slightly eccentric (Nesvorný 2015). A scenario with a local formation of the CCKB and an episode of an eccentric Neptune was also checked by this author in previous numerical simulations (Gomes et al. 2018) and no DCP was detected in the data from those simulations. This is expected since the relative

excitation of the CCKB induced by an eccentric Neptune is provoked by pure secular dynamics with no close encounter episodes that could at least moderately scatter the planetesimals from the primordial CCKB. Also in a scenario where Neptune always or mostly migrates with low eccentricity (Nesvorný 2015) there is always a 'migrating' scattered population with Neptune but no mechanism to detach them to larger perihelia keeping low inclinations, since there is a void of important MMRs with Neptune just past the 2:1 MMR with Neptune and classical mechanisms that produce the detached objects require important MMRs with Neptune and a fairly high planetesimal's inclination to allow for the coupled MMR Kozai mechanism that increases the planetesimal's perihelion distance with a simultaneous inclination increase.

Even though streaming instability theories have given a large step towards explaining the formation of large planetesimals from a small amount of mass in pebbles, it is still questionable whether the right conditions in the primordial solid-gas disk was attained to form the objects in the present CCKB. The short range transport scenario here presented may eventually show to be compatible to more realistic conditions for the primordial gas-solids disk, since the objects as large as those found in the CCKB primordially in the OBD would sum to a total mass of 20-100 times the present CCKB mass.

Finally, although the scenario here presented dispenses a local formation for the CCKB it is however not incompatible with an in situ formation of part of the CCKB. In this case a fraction of the CCKB would have a local formation and another part would have been transported. There might be then some small differences in the physical characteristics of those two subpopulations. Possibly the local formed objects would belong to the reddest classes. It is however noteworthy that three of the detached low inclination objects above mentioned, 2001

UR163, 1995 TL8 and 2002 GZ31, have their B-R magnitudes in the range 1.75 to 1.97, two

of them belonging to the RR class, thus already pushed towards very red objects.

## REFERENCES

- Brasil, P. I. O., Gomes, R. S., & Soares, J. S. 2014a, *A&A*, 564, A44
- Brasil, P. I. O., Nesvorný, D., & Gomes, R. S. 2014b, *AJ*, 148, 56
- Dawson, R. I., & Murray-Clay, R. 2012, *ApJ*, 750, 43
- Drażkowska, J., & Dullemond, C. P. 2014, *A&A*, 572, A78
- Edgeworth, K. E. 1949, *MNRAS*, 109, 600
- Fraser, W. C., Brown, M. E., Morbidelli, A., Parker, A., & Batygin, K. 2014, *ApJ*, 782, 100
- Gomes, R., Levison, H. F., Tsiganis, K., & Morbidelli, A. 2005, *Nature*, 435, 466
- Gomes, R., Nesvorný, D., Morbidelli, A., Deienno, R., & Nogueira, E. 2018, *Icarus*, 306, 319
- Gomes, R. S. 1997, *AJ*, 114, 2166
- . 2000, *AJ*, 120, 2695
- . 2003, *Icarus*, 161, 404
- . 2011, *Icarus*, 215, 661
- Gomes, R. S., Morbidelli, A., & Levison, H. F. 2004, *Icarus*, 170, 492
- Johansen, A., Oishi, J. S., Mac Low, M.-M., et al. 2007, *Nature*, 448, 1022
- Kenyon, S. J., & Luu, J. X. 1999, *AJ*, 118, 1101
- Kuiper, G. P. 1951, *Proceedings of the National Academy of Science*, 37, 1
- Levison, H. F., & Morbidelli, A. 2003, *Nature*, 426, 419
- Levison, H. F., Morbidelli, A., Van Laerhoven, C., Gomes, R., & Tsiganis, K. 2008, *Icarus*, 196, 258
- Lykawka, P. S., & Mukai, T. 2007, *Icarus*, 192, 238
- Malhotra, R. 1995, *AJ*, 110, 420
- Morbidelli, A., & Nesvorný, D. 2020, *Kuiper belt: formation and evolution*, ed. D. Prialnik, M. A. Barucci, & L. Young, 25–59
- Nesvorný, D. 2011, *ApJL*, 742, L22
- . 2015, *AJ*, 150, 68
- Nesvorný, D., Li, R., Youdin, A. N., Simon, J. B., & Grundy, W. M. 2019, *Nature Astronomy*, 3, 808
- Nesvorný, D., & Morbidelli, A. 2012, *AJ*, 144, 117
- Nesvorný, D., Vokrouhlický, D., Alexandersen, M., et al. 2020, *arXiv e-prints*, arXiv:2006.01806
- Parker, A. H., & Kavelaars, J. J. 2010, *ApJL*, 722, L204
- Ribeiro de Sousa, R., Gomes, R., Morbidelli, A. r., & Vieira Neto, E. 2019, *Icarus*, 334, 89
- Tsiganis, K., Gomes, R., Morbidelli, A., & Levison, H. F. 2005, *Nature*, 435, 459
- Ward, W. R., & Canup, R. M. 2006, *Science*, 313, 1107
- Youdin, A. N., & Goodman, J. 2005, *ApJ*, 620, 459